# Convolutional Neural Networks for Non-parasitic Nematode Feeding Behavior Identification in Soil Ecosystem Management

Nabila H. Shabrina [1,*], Larasati[1], Siwi Indarti [2], and Rina Maharani [2]

[1] Department of Computer Engineering, Faculty of Engineering and Informatics, Universitas Multimedia Nusantara, Tangerang, Indonesia

[2] Department of Plant Protection, Faculty of Agriculture, Universitas Gadjah Mada, Sleman, Indonesia

Email: nabila.husna@umn.ac.id (N.H.S.); larasati@student.umn.ac.id (L.); siwi.indarti@ugm.ac.id (S.I.); rina.maharani@mail.ugm.ac.id (R.M.)

*Corresponding author

***Abstract*—Non-parasitic nematodes play a critical role in maintaining soil health and promoting crop productivity. Recognizing these roles is essential for developing effective and targeted strategies for sustainable farming. Valuable insights into the functional role of nematodes in soil can be obtained by categorizing them into bacterial feeders, fungal feeders, and the predatory-omnivorous group. However, traditional identification methods based on visual taxonomic traits are challenging and time-consuming. Advancements in artificial intelligence, particularly deep learning, have opened new frontiers in nematode identification; however, studies focusing on non-parasitic nematodes and their feeding behaviors remain limited. This study bridges this gap by leveraging state-of-the-art Convolutional Neural Network (CNN) architectures to classify non-parasitic nematodes from a small dataset of 921 microscopic photographs collected from agricultural fields and labeled according to their feeding habits. Ten CNN architectures, including Xception, VGG16, ResNet50, InceptionV3, InceptionResNetV2, NASNetMobile, DenseNet121, DenseNet201, EfficientNetV2B0, and ConvNeXtTiny, were evaluated for their performance. Among these, DenseNet121 emerged as the top performer, achieving a test accuracy of 0.86. These findings highlight the potential of deep learning-based techniques to revolutionize soil health management by enabling precise and efficient identification of nematodes.**

***Keywords*—Convolutional Neural Networks (CNN), deep learning, non-parasitic nematode, precision agriculture, soil management**

## I. Introduction

Nematodes are microscopic, ubiquitous, and highly diverse smooth-skinned roundworms that inhabit diverse ecosystems across all climatic zones, from marine and freshwater environments to terrestrial soil [1]. Their broad distribution and vital role in nutrient recycling make them one of the most thoroughly examined groups of soil bioindicators [2]. Non-parasitic nematodes occupy various soil niches, feeding on bacteria and fungi or preying on other small organisms [3]. Through these feeding activities, they influence soil health, nutrient dynamics, and ecosystem balance, while also serving as sensitive indicators of pollution and environmental disturbances [4]. Accurate identification of non-parasitic nematodes is therefore essential for agricultural management, as their feeding habits affect soil fertility, crop productivity, nutrient cycling, and pest control [5, 6].

Non-parasitic nematodes, classified by feeding type as bacterivores, fungivores, and omnivorous–predators, provide valuable insights into soil function. The dominance of bacterivores often reflects rapid nutrient cycling driven by bacterial decomposition, which is typically associated with high nitrogen input or recent tillage [7, 8]. In contrast, fungivore prevalence indicates a fungi-based food web with slower nutrient turnover and relatively undisturbed soil [9]. Omnivorous and predatory nematodes are markers of more complex soil food webs; low populations may suggest disturbance, contamination, or excessive fertilizer use, whereas higher abundance generally signals biodiversity and the capacity to regulate plant-parasitic nematodes and other pathogens [10].

Identifying the feeding habits of nematodes involves examining their morphological features, including mouthparts, body length, sexual organs, specific characteristics of the body part, tail, and other physical attributes, as observed under a microscope [11]. However, their small size (approximately 500 μm in body size) and the limited distinctiveness of traits across many functionally diverse taxa make their accurate identification difficult [12]. Conventional identification by experts using microscopy photographs is time-consuming and prone to inconsistent outcomes, particularly when dealing with a large number of samples. This highlights the need for a rapid and reliable method for identifying non-parasitic nematodes.

Manuscript received July 25, 2025; revised August 13, 2025; accepted September 26, 2025; published February 27, 2026.

Remarkable progress in artificial intelligence, particularly in machine learning and deep learning, has significantly influenced numerous scientific disciplines [3]. Among these, deep learning has proven to be outstanding in various applications [13]. Deep learning has shown great potential in the agricultural sector, including crop yield projections, plant stress identification, weed and pest detection, disease diagnosis, and intelligent farming practices [14–18]. Convolutional Neural Network (CNN), a deep learning model specifically designed for photograph data, can automatically learn the spatial hierarchies of features, making it highly effective for analyzing visual data [19]. Their ability to perform automatic feature extraction has been successfully applied in agricultural contexts, such as plant disease identification [20–24]. CNN are increasingly applied to nematode identification, as they can effectively capture and analyze key morphological features critical for accurate identification.

Recent advances have enabled nematode detection at the field scale, for example, through drone-based spectral analysis of soybean cyst nematodes and hyperspectral or remote sensing approaches for plant-parasitic nematodes [25–27]. These methods demonstrate the feasibility of large-scale monitoring but remain focused on detecting or quantifying plant-parasitic nematodes. In contrast, post-extraction analysis of soil, root, or water samples using microscopic imaging combined with deep learning provides the opportunity to perform specimen-level classification based on morphological traits that are not accessible through field-scale analyses. Most existing deep learning applications for nematode identification have focused on parasitic nematodes [28–33]. To the best of our knowledge, Uhlemann *et al*. [34] conducted the only study utilizing a dataset of non-parasitic nematodes; however, their approach was limited to genus-level identification and did not extend to classification by feeding type.

To build upon previous research and provide a novel approach for assessing soil nematodes, this study proposes a novel deep learning-based approach that utilizes CNN to classify non-parasitic nematodes by their feeding types. A dataset of 921 microscopic photographs sourced from agricultural fields in Indonesia was analyzed using ten state-of-the-art Convolutional Neural Network architectures, including Xception, VGG16, ResNet50, InceptionV3, InceptionResNetV2, NASNetMobile, DenseNet121, DenseNet201, EfficientNetV2B0, and ConvNeXtTiny, and each algorithm was fine-tuned to achieve optimal performance [35–44]. The results of our experiments are documented in this paper, and the performance of each algorithm is compared using several evaluation metrics, including accuracy, F1-Score, precision, and recall.

The key contributions of this study are as follows:

- This study introduces fine-tuned CNN architectures capable of accurately and quickly classifying non-parasitic nematodes based on their feeding behaviors;
- Creation of an automatic identification system leveraging DenseNet121, which achieved superior results in terms of accuracy and other key performance metrics.

## II. Literature Review

Several studies have demonstrated the successful implementation of deep learning, specifically Convolutional Neural Network, for nematode identification [11]. Uhlemann *et al*. [34] showed that the Xception model is effective in identifying both juvenile and adult nematode stages. Contrary to the model utilizing randomly initialized weights, the pre-trained model exhibited superior performance, resulting in average validation accuracies of 88.28% and 69.45% for the juvenile and adult datasets, respectively. Lu *et al*. [45] focused on publicly available nematode datasets and provided a benchmark by evaluating several deep learning models on these datasets. The dataset comprised 2769 manually classified nematode samples from 19 classes. The results revealed that the ResNet model achieved the highest accuracy of 79%. NemaNet was proposed by Abade et al. to identify nematode datasets in soybean plants in Brazil, and it demonstrated an accuracy of 96.99% [33]. Angeline *et al*. [46] explored the application of CNNs for the detection of parasitic and non-parasitic nematodes in soil samples. This study utilized a faster region-based CNN to analyze microscope photographs of soil samples and achieved an accuracy of 87.5%.

Shabrina *et al*. [30] collected a dataset of plant-parasitic nematodes commonly found in Indonesia and tested several advanced deep learning models, including CoAtNet-0, ResNet101V2, EfficientNetV2B0, and EfficientNetV2M, to identify plant-parasitic nematodes in this dataset. The models were assessed using various optimization function and augmentation technique configurations. The results revealed that the EfficientNetV2B0 and EfficientNetV2M models yielded the highest accuracy of 97.94% on the test dataset. In addition, Shabrina *et al*. [31] compared 15 popular CNN models for identifying phytoparasitic nematodes from microscopic photographs. The results indicated that CoAtNet-0 exhibited the best performance, with a test accuracy of 98.06%.

Agarwal *et al*. [47] made available a new public dataset featuring annotated photographs of plant-parasitic nematodes obtained through heterologous soil extractions. This dataset can aid in the rapid identification of nematodes using several deep learning object detection models. The study outcomes revealed that YOLOv5 delivered the most impressive performance, attaining a peak mean Average Precision (mAP) of 0.787 at 0.5 Intersection over Union (IoU). Pun *et al*. [48] used the architectures of YOLO versions two to seven to explore root knot nematode enumeration in microscopic photographs. The authors enhanced the performance of YOLOv5 by employing mosaic augmentation, resulting in a precision of 1.00, recall of 0.998, F1-Score of 0.999, and mAP of 0.995 [48].

## III. Materials and Methods

### A. Research Workflow

Fig. 1 depicts the workflow for creating an automatic system for non-parasitic nematode identification. This process began with data collection from agricultural land in Indonesia. The collected data were preprocessed by converting the color format to RGB, resizing the photographs, and applying data augmentation. The preprocessed photographs were subsequently used as inputs to train the CNN model. The results were documented and analyzed to determine the best-performing CNN model. Owing to the small size of the datasets, the CNN model was implemented using a transfer learning approach, in which a pretrained model was employed as the basis for training a new model on a related dataset [49]. The best model was then deployed in a user-friendly application, ensuring ease of use for end users.

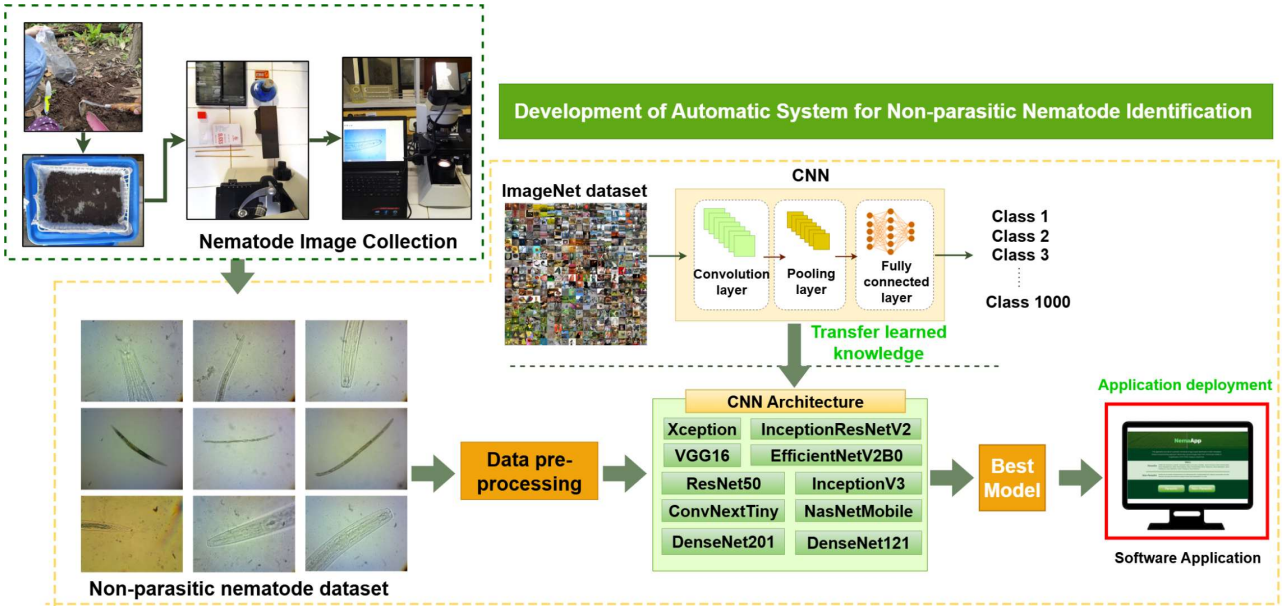


Fig. 1. Overall research workflow for developing an automatic system for non-parasitic nematode identification. The workflow starts with nematode photograph collection, followed by the creation of a non-parasitic nematode dataset. Data preprocessing was used to prepare the photographs for training multiple CNN architectures. Transfer learning from ImageNet pre-trained models was then applied, and the best-performing model was selected for deployment as a software tool.

### B. Materials

#### 1) Data collection

During data collection, we used a random sampling method to gather samples from eight distinct vegetation types in Yogyakarta and Central Java, Indonesia, which represent various soil management practices. The Whitehead-Tray extraction method, as modified by Coyne *et al*. [50], was employed to extract nematodes from the soil. Soil samples were collected from each vegetation layer at a depth of 0–20 cm. From 5–10 cores, the samples were subsequently compounded, and nematodes were selected before being placed on glass slides with 20 µL of sterilized water. Subsequently, photographs of non-parasitic nematodes were captured using an Olympus CX- 31 binocular microscope equipped with 400–1000× magnification and an OptiLab Miconos optical camera. The captured photographs were then labelled by two nematologists from the Department of Plant Protection, Faculty of Agriculture, Universitas Gadjah Mada, Indonesia.

Nematologists have identified nematode genera based on their morphology by carefully observing their physical characteristics, such as the length and shape of their bodies, morphology of their sexual organs, and appearance of their mouth and tail parts. Each individual was observed under a microscope before capturing photographs. Following this observation, the nematode sample was captured in several photographs for each nematode, including pictures of the mouth, tail, sexual organs, and full-body shape.

The dataset included nematode orders Rhabditida and Tylenchida, represented by the following genera: Acrobeles, Acrobeloides, Rhabditis, Aphelenchus, and Tylenchus. Additionally, the dataset included nematode orders Dorylaimida and Mononchida. The dataset was divided into three categories based on feeding habits: bacterivores, fungivores, and predator–omnivores. Predators and omnivores were grouped into one class because some families of nematodes have feeding habits that are both predatory and omnivorous [51]. Based on their morphology, the predators were divided into two groups: “ingesters” with wide stoma, and as “piercers” with a narrow stylet to suck the body fluids. The piercer group of predators had a morphology similar to that of the omnivores. Piercer predators, such as Labronema, are included in the Dorylaimidae Family, whereas some other genera in this family are also omnivores. Additionally, predators and omnivores share similar colonizer-persister (c-p) values ranging from 4 to 5, indicating that they possess long life cycles and are sensitive to disruptions in their life strategies [52].

The numbers of photographs for each category were 287, 80, and 554 for bacterivores, fungivores, and predator–omnivores, respectively. The dataset was divided into two parts: a training set and a testing set, where the training set comprised 90% of the data, and the testing set consisted of 10%. In addition, 10% of the training set was used for validation. The dataset was considered to have an imbalanced distribution of photographs because there was a significant difference in the number of photographs among the bacterivore, fungivore, and predator-omnivore categories. This imbalance is attributed to the availability of nematodes in the field, which is influenced by environmental conditions, farming practices, the presence of host plants, and abiotic and biotic soil factors, such as pH, temperature, relative humidity, organic content, and other organisms [53]. To address this, we applied data augmentation to balance the training dataset. The details of these methods are described in the following sections.

During our observations, we encountered only one order of predators and one order of omnivorous nematodes in the field. Similarly, only two genera of fungivore nematodes have been identified in the field. The fungivore nematode class had a comparatively small number of photographs because of its limited occurrence in the field. Despite this, the current dataset includes a range of nematode genera commonly found in Indonesia and other tropical regions. To maintain ecological relevance and prevent potential biases, we chose not to incorporate additional external datasets. This approach ensured that the dataset accurately represented real-world field conditions, while optimizing computational efficiency.

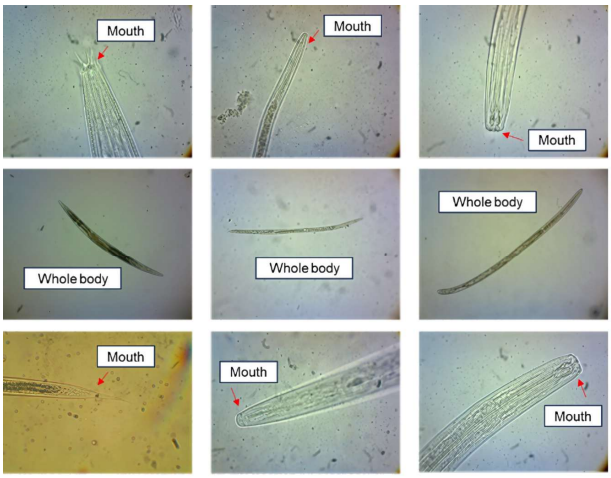


(a) Bacterivore (b) Fungivore (c) Predator-omnivore

Fig. 2. Representative samples from the non-parasitic nematode dataset. Photographs categorized by feeding behavior: (a) bacterivores, (b) fungivores, and (c) predator-omnivores. Photographs were obtained using light microscopy at 40× magnification, showing either whole-body or partial views (e.g., mouth regions) to highlight the key morphological features relevant to nematode identification.

The sample datasets for each class are shown in Fig. 2. Bacterivores, including Acrobeles, Acrobeloides, and Rhabditis, are characterized by a hollow tube-like mouth or stoma designed to swallow bacteria. Fungivores, such as Aphelenchus and Tylenchus, are equipped with stylets that lack a knob or have a weak knob, which they use to pierce fungal hyphae. They also had a tapered body with a metacorpus and valve. Predatory nematodes may have large mouths and immobile teeth. Both predator and omnivorous bodies were relatively large. Predators, such as those in the order of Mononchida, have a cylindrical esophagus and an open-shaped stoma cuticularized with one or two obvious teeth. Dorylaimida, an omnivore, is characterized by a feeding spear or odontostyle [54].

*2) Data pre-preprocessing*

Fig. 3 illustrates the preprocessing methods used for the dataset. Original microscopic photographs with dimensions of 2560×2048 and 4100×3075 pixels were used. Owing to the variation in color formats in the collected dataset, the photographs were converted to the RGB color format to ensure uniformity. Pixel scaling was implemented to simplify the computational process and accelerate model convergence. This involved resizing photographs to match the input shape requirements of each model. Photograph resizing was designed to meet most of the CNN models, with an input size of 224×224 pixels, except for Xception, InceptionV3, and InceptionResnetV2, which had larger input sizes of 299×299 pixels.

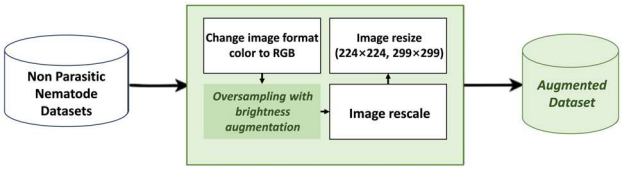


Fig. 3. Data pre-processing steps.

Brightness augmentation was applied because of the imbalanced number of photographs in the dataset. This technique was proven to be effective based on the findings of previous studies, which demonstrated that implementing brightness augmentation could enhance the performance of the trained model [30, 55, 56]. Brightness augmentation was applied with a range from 0.1 to 1.0, signifying the degree to which the brightness of the photographs was randomly elevated. This augmentation was performed in an oversampling scenario, in which the number of photographs per class was increased until it reached the highest quantity for the class within the training set, with a value of 449. This number was chosen because of the limited computational resources of our system. Augmentation was applied only to the training set, whereas the validation and testing sets were left unaltered to ensure an unbiased evaluation of the model performance.

Subsequently, the photographs were resized using a scaling factor of 1/255. This adjustment was necessary to ensure that the pixel values were within the algorithm range. By dividing each pixel value by 255, the original range of 0–255 was transformed into 0–1, thus aligning the pixel representations with the expected value range. This adjustment is crucial for facilitating further processing or training procedures because it ensures that the pixel values are appropriately scaled to meet the specific requirements of the algorithm.

## C. Methods

### 1) Convolutional Neural Networks (CNN) architecture

CNN are advanced algorithms with exceptional performance in the field of computer vision. The architecture of a CNN comprises an input layer, convolution layers, pooling layers, and fully connected layers, culminating in an output layer (Fig. 4). The input layer was designed to access the spatial data from the photograph. The convolutional layer, which follows the input layer, is primarily responsible for extracting features from the input photograph while maintaining the spatial relationships between pixels. It applies to a set of kernels (filters) that slide across the entire photograph, computing local dot products at each position to detect patterns such as edges, textures, and shapes. These feature maps capture both low-level and high-level representations of the input and are often followed by a pooling layer to further reduce the dimensionality. The pooling layer decreases the spatial dimensions of the feature maps while preserving the vital information. This minimizes computational complexity and prevents overfitting. The final layer is often a fully connected layer that is utilized for specific tasks, such as classification, where the aim is to predict the class or category of the input data. A key feature of CNNs is their substantial capacity for processing complex information. This feature makes CNNs an ideal choice for image identification and classification tasks. CNNs can serve as viable alternatives for nematode identification because of their ability to handle complex morphological characteristics.

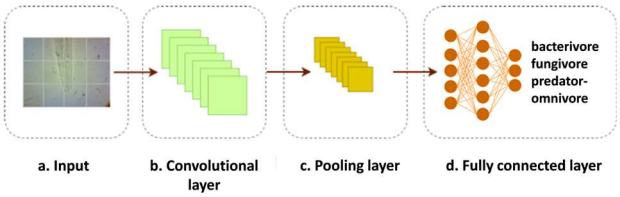


Fig. 4. Basic structure of a CNN for nematode feeding behavior classification. (a) Input: microscopic photographs of nematodes; (b) convolutional layer: filters applied to extract local features; (c) pooling layer: down-sampling to reduce dimensionality while retaining key features; and (d) fully connected layer: final classification into bacterivore, fungivore, and predatory-omnivorous groups.

### 2) Transfer Learning (TL)

Owing to the limited data, this study employed Transfer Learning (TL) to train the CNN model. TL aims to enhance the comprehension of the present task by connecting it to other tasks executed at various points in time using a relevant source. TL is especially beneficial in situations where specific training data are scarce. By utilizing TL, the time, cost, and resources required to train a model can be significantly reduced. TL can be utilized using several pre-trained models that can be run using simple devices with limited processing and training times. A pretrained model is a deep learning model trained on a large dataset to understand general features or representations. Once trained, the weights and parameters of the model were saved and transferred for use on other datasets. This pretrained model can also be adjusted for a specific task and used to extract features from a smaller dataset.

This study aimed to create a novel application utilizing transfer learning on several pretrained CNN models for non-parasitic nematode identification. As illustrated in Fig. 5, the CNN was pretrained to categorize 1000 classes derived from the ImageNet dataset [57]. The learned knowledge was then transferred to learn the features of the non-parasitic nematode dataset. In this study, we modified the final layer of a pre-existing network and refined it to categorize three types of non-parasitic nematode feeding behaviors. The final layer was substituted with two-level layers of a fully connected network that included dropout, ReLU activation and a softmax layer [58, 59].

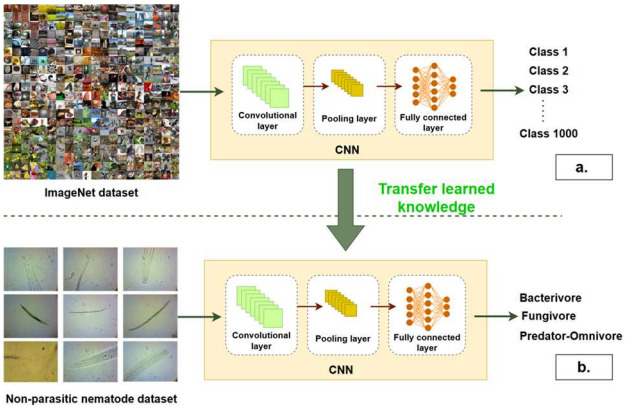


Fig. 5. Illustration of the transfer learning approach used in this study. (a) A CNN is first trained on the large-scale ImageNet dataset, where the convolutional and pooling layers extract generic visual features across 1000 classes. (b) The pre-trained network was then fine-tuned on the non-parasitic nematode dataset, transferring the learned features to classify nematodes into bacterivore, fungivore, and predatory-omnivorous groups.

TABLE I. COMPARISON OF THE PARAMETERS OF THE APPLIED CNN

| Models | Total Parameters | Layers |
|---|---|---|
| Xception | 20,861,480 | 132 |
| VGG16 | 14,714,688 | 19 |
| ResNet50 | 23,587,712 | 170 |
| InceptionV3 | 21,802,784 | 311 |
| InceptionResNetV2 | 54,336,736 | 780 |
| NasnetMobile | 4,269,716 | 769 |
| DenseNet121 | 7,037,504 | 427 |
| DenseNet201 | 18,321,984 | 707 |
| EfficientNetV2B0 | 5,919,312 | 270 |
| ConvNextTiny | 27,820,128 | 151 |

In this study, ten variants of pre-trained CNN architectures were implemented: Xception , VGG16 , ResNet50, InceptionV3, InceptionResNetV2, NASNetMobile, DenseNet121, DenseNet201, EfficientNetV2B0, and ConvNeXtTiny [35–44]. The selection of CNNs for the classification of non-parasitic nematodes is influenced by the availability of resources and the desire to achieve an optimal balance between accuracy and computational efficiency of the model. Because the dataset consisted of high-resolution photographs, we selected ten CNN architectures that demonstrated strong performance on the ImageNet benchmark while being relatively resource-efficient [60]. These pretrained models were subsequently fine-tuned on

our labeled nematode dataset. The parameters of the applied CNNs, including the number of parameters and fine-tuning layers, are listed in Table I for comparison purposes.

*3) Hyperparameter settings*

Successful transfer learning implementation requires tailored adjustments and strategies that cater to various scenarios, including the optimization of the hyperparameter settings. Hyperparameter settings play a critical role in the training process and must be set appropriately to achieve optimal results [61]. To ensure a fair and consistent evaluation, the same hyperparameters were applied to all models. A Stochastic Gradient Descent (SGD) optimizer was used with a learning rate of 0.001. SGD is a widely used optimization algorithm that requires an entire training dataset for each weight update. As the dataset size increases, the computational demands also increase. However, SGD uses a batch of data corresponding to the chosen batch size for each weight update, thereby allowing more frequent updates with smaller data subsets. This enhances computational efficiency and facilitates the optimization process for larger datasets, making it faster and more feasible [33]. Additionally, previous studies have shown that the SGD optimizer is more effective than other optimization techniques, such as Adam and RMS, for nematode classification tasks [30, 56]. All CNN models were trained with a batch size of 32 for up to 50 epochs using categorical cross-entropy as the loss function. An early stopping technique with a patience of five was applied to prevent overfitting, and dropout rates of 0.5 and 0.3 were implemented across the models.

*4) Deployment*

A software application that integrates a CNN model was deployed to automate the identification and classification of nematode feeding behaviors. This process involves the smooth integration of the best-performing model using Flask, a lightweight and efficient framework developed in the Python programming language, as illustrated in Fig. 6.

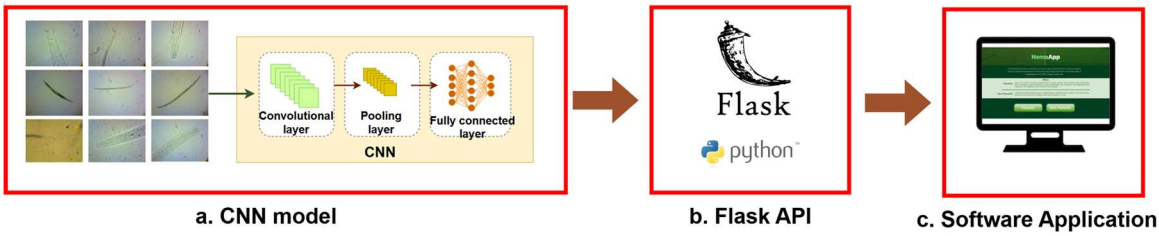


Fig. 6. Deployment workflow of the trained CNN model for non-parasitic nematode classification. (a) The trained CNN model, (b) Flask API implemented in Python for deploying the model, and (c) the software application interface that delivers classification results to end-users.

*5) Implementation and evaluation*

The training process was performed on a computer equipped with an 11th Intel Core i7-11800H processor, NVDIA GeForce RTX 3070 Max-Q 8GB GDDR6, with 16 GB of memory. The code implementation was primarily performed using the Keras and TensorFlow libraries. Evaluation metrics play a crucial role in gauging the ability of a model to accurately and effectively predict the unseen data in a test dataset. In this study, various evaluation metrics, including accuracy, precision, recall, and F1-Score, were used to comprehensively assess the model predictions. The accuracy rate was calculated by dividing the total number of correctly predicted instances by the total number of samples evaluated. This metric provides a comprehensive understanding of the capacity of the model to accurately predict both the positive and negative classes. The equation for this metric is expressed in Eq. (1).

$$Accuracy = \frac{TP + TN}{TP + TN + FP + FN} \quad (1)$$

Precision evaluates the proportion of correct predictions made by a model for the positive class relative to all positive predictions. A higher precision value indicates a lower number of incorrect positive classifications. This metric primarily concerns the accuracy of positive classifications and is particularly relevant when the cost of false negatives is significant. The equation for precision is given in Eq. (2).

$$Precision = \frac{TP}{TP + FP} \quad (2)$$

Recall/sensitivity is the percentage of correctly classified positive samples. This metric evaluates a model's capability to identify all positive instances within a class and is calculated separately for each class. A higher recall value signifies that a greater proportion of positive samples has been accurately identified by the model, and this is particularly significant when the cost of false negatives is significant. Eq. (3) shows the recall formula.

$$Recall = \frac{TP}{TP + FN} \quad (3)$$

The F1-Score offers a comprehensive assessment of a model's ability to correctly classify positive samples while also identifying all positive instances. The F1-Score is a valuable metric that considers both false positives and false negatives and is particularly useful in situations where there is an unbalanced distribution of classes or when both precision and recall are of equal importance. A higher F1-Score indicates a better balance between

precision and recall and signifies a strong overall model performance. The formula for F1-Score is given in Eq. (4).

$$F1-Score = 2 \times \frac{Precision \times Recall}{Precision + Recall} \quad (4)$$

All metrics are represented by four possible outcomes: True Positive (TP), False Positive (FP), False Negative (FN), and True Negative (TN).

## IV. Result

### A. Model Performance Results

To provide a more rigorous estimate of performance reliability, 95% confidence intervals were calculated for each metric using a bootstrap resampling procedure with 1000 iterations. In this procedure, the test set was resampled with replacement, and the performance metrics were recalculated for each iteration. The results distribution was reported as the lower and upper bounds of the confidence intervals.

According to the data presented in Table II, the DenseNet121 model achieved the best performance in all metric evaluations, with a test accuracy of 0.86 (95% CI: 0.80–0.93). Because of the balanced number of photographs in the augmented dataset, the precision, recall, and F1-Score were calculated using a macro-average, which treats all classes equally. DenseNet 201 achieved the highest precision of 0.77 (95% CI: 0.68–0.93). The highest recall was achieved with a value of 0.75 (95% CI: 0.64–0.93) by DenseNet121. The highest F1-Score was achieved by DenseNet121, with a value of 0.75 (95% CI: 0.64–0.87). The ResNet50 model had the lowest test accuracy in the augmented dataset (0.11). EfficientNetV2B0 and ConvNeXtTiny, which performed poorly on the original dataset, also exhibited poor performance on the augmented dataset, with test accuracies of 0.31 and 0.6, respectively. This suggests that the architectures of the EfficientNetV2B0, ResNet50, and ConvNeXtTiny models did not align with the features that should be extracted from non-parasitic nematodes.

TABLE II. Comparison of Model Performance Result

| Model | Test accuracy (95% CI) | Precision (95% CI) | Recall (95% CI) | F1-Score (95% CI) |
|---|---|---|---|---|
| Xception | 0.83 (CI: 0.73–0.88) | 0.75 (CI: 0.57–0.87) | 0.75 (CI: 0.57–0.87) | 0.74 (CI: 0.57–0.82) |
| VGG16 | 0.71 (CI: 0.63–0.82) | 0.65 (CI: 0.54–0.79) | 0.75 (CI: 0.63–0.88) | 0.65 (CI: 0.54–0.72) |
| ResNet50 | 0.11 (CI: 0.11–0.11) | 0.36 (CI: 0.36–0.36) | 0.35 (CI: 0.35–0.35) | 0.08 (CI: 0.08–0.08) |
| InceptionV3 | 0.81 (CI: 0.71–0.86) | 0.69 (CI: 0.58–0.88) | 0.68 (CI: 0.51–0.78) | 0.68 (CI: 0.52–0.79) |
| InceptionResNetV2 | 0.70 (CI: 0.57–0.83) | 0.63 (CI: 0.56–0.82) | 0.60 (CI: 0.51–0.80) | 0.61 (CI: 0.56–0.81) |
| NASNetMobile | 0.78 (CI: 0.72–0.88) | 0.71 (CI: 0.62–0.86) | 0.70 (CI: 0.61–0.85) | 0.71 (CI: 0.61–0.85) |
| DenseNet121 | **0.86 (CI: 0.80–0.93)** | 0.75 (CI: 0.65–0.91) | **0.75 (CI: 0.64–0.87)** | **0.75 (CI: 0.64–0.87**) |
| DenseNet201 | 0.84 (CI: 0.76–0.91) | **0.77 (CI: 0.68–0.93)** | 0.72 (CI: 0.63–0.88) | 0.74 (CI: 0.65–0.88) |
| EfficientNetV2B0 | 0.31 (CI: 0.31–0.31) | 0.10 (CI: 0.10–0.10) | 0.33 (CI: 0.33–0.33) | 0.16 (CI: 0.16–0.16) |
| ConvNeXtTiny | 0.60 (CI: 0.60–0.60) | 0.20 (CI: 0.20–0.20) | 0.33 (CI: 0.33–0.33) | 0.25 (CI: 0.25–0.25) |

### B. Accuracy and Loss Curves

The evaluation of the accuracy and loss curves is important for assessing the performance of the CNN model. These curves are useful as instruments for surveilling the metamorphosis of the accuracy and loss metrics during the training process, providing a comprehensive understanding of the learning evolution of the CNN and enabling the detection of any conceivable issues in the model. The accuracy and loss curves of the CNN demonstrate the model's ability to classify non-parasitic nematodes and its progress in minimizing errors during training as epochs advance. Most curves demonstrate the increasing accuracy of the CNN, as it correctly classifies more nematodes and its decreasing loss as it becomes more accurate. The learning curve is shown for a maximum of 15 epochs because most of the models were stopped around 13–17 due to the implementation of the early stopping technique. During the initial epoch, all CNN models progressed their accuracy in both training and validation, followed by a more static improvement in the final epoch. The loss training and validation curves showed that the initial loss was high and then degraded as the number of epochs increased. The data suggest that most CNN models can learn effectively from the data and improve their performance throughout the training process.

Figs. 7 and 8 show the training and validation accuracy curves of the evaluated CNN architectures. Xception, Inception-based models, and DenseNet architecture consistently surpassed 80% accuracy, reflecting their strong capacity to learn discriminative features and generalize effectively to new data.

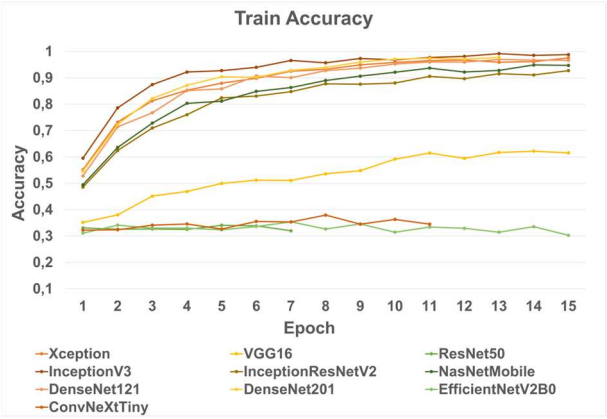


Fig. 7. Training accuracy over 15 epochs for ten convolutional neural network architectures applied to non-parasitic nematode classification.

VGG16 demonstrated moderate performance, stabilizing between 70% and 80% validation accuracy, whereas ResNet50 and EfficientNetV2B0 exhibited

slower convergence and limited adaptability. In contrast, NasNetMobile and ConvNeXtTiny underperformed markedly, with ConvNeXtTiny failing to exceed 40% accuracy in the training and validation sets. These results highlight the superiority of advanced architectures, such as Xception and DenseNet, for non-parasitic nematode identification.

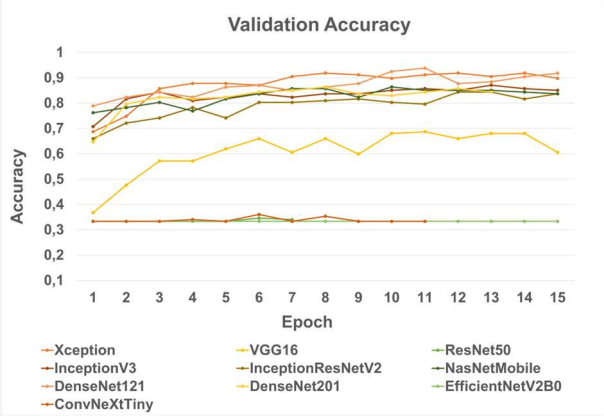


Fig. 8. Validation accuracy curves over 15 epochs for ten convolutional neural network architectures applied to non-parasitic nematode classification.

Figs. 9 and 10 illustrate the training and validation loss curves, providing insights into the convergence dynamics and model stability. Xception, Inception-based models, and DenseNet architectures achieved rapid and smooth loss reduction, stabilizing at approximately 0.1, indicative of efficient optimization with minimal overfitting. VGG16 attained moderate convergence but plateaued at higher loss values, whereas ResNet50 and EfficientNetV2B0 stabilized at approximately 0.4–0.5, suggesting suboptimal learning efficiency. In contrast, NasNetMobile and ConvNeXtTiny exhibited persistently high losses, with ConvNeXtTiny remaining above 1.0 throughout the training, underscoring its inadequate learning capacity. Collectively, these results confirm that Xception, DenseNet, and Inception-based models are not only more accurate but also more stable in terms of their convergence behavior than the other evaluated architectures.

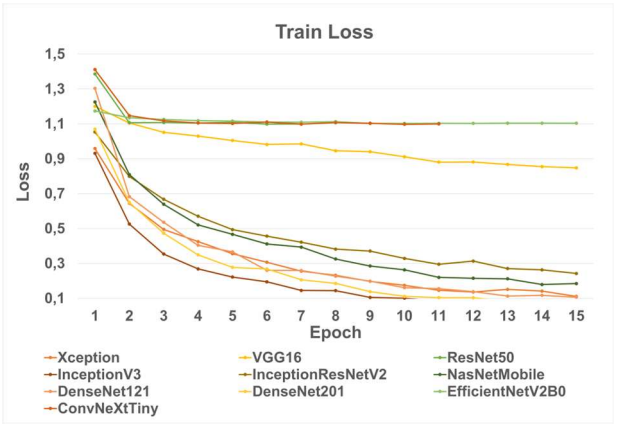


Fig. 9. Training loss curves over 15 epochs for ten convolutional neural network architectures trained on the augmented non-parasitic nematode dataset.

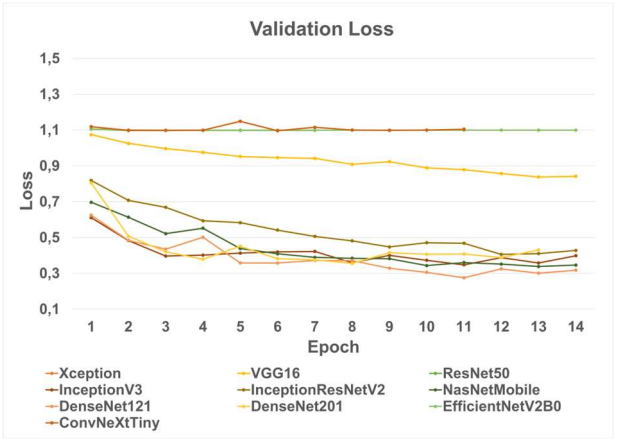


Fig. 10. Validation loss curves over 15 epochs for ten convolutional neural network architectures trained on the augmented non-parasitic nematode dataset.

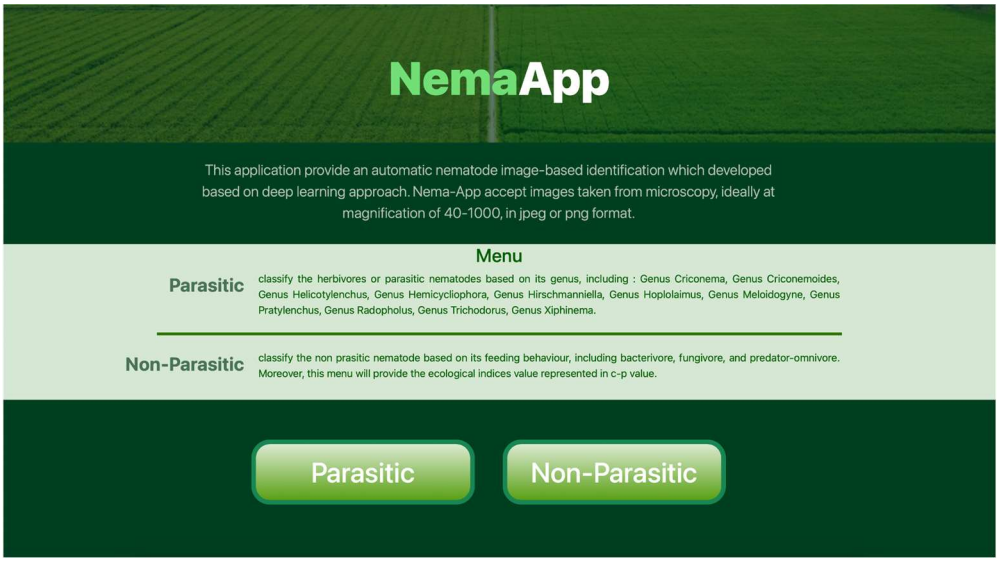


Fig. 11. User interface of Nema-App.

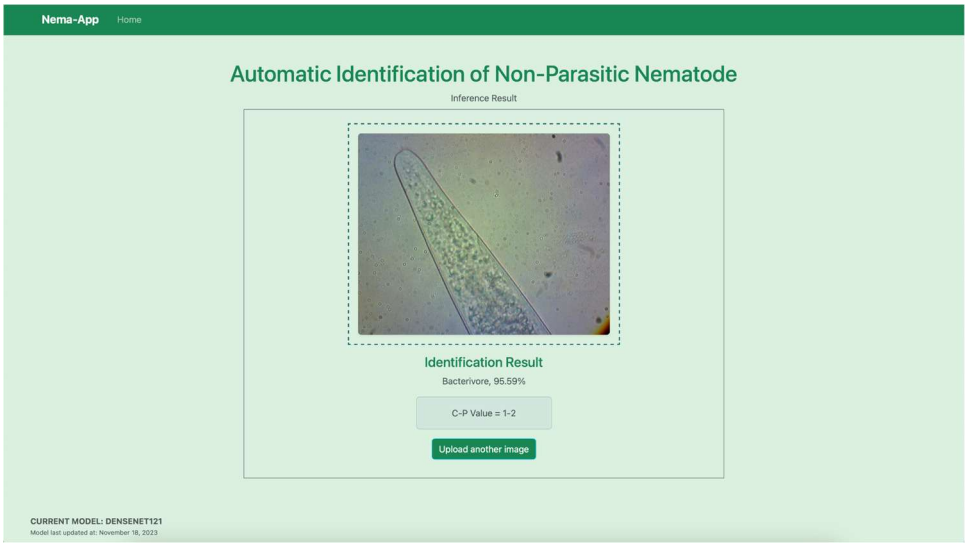


Fig. 12. Sample results of Nema-App.

### C. Deployment of the Non-Parasitic Nematode Identification Software

The final output of this study offers a deployed deep learning model in the form of a desktop application that can be easily utilized by prospective agriculturalists. By creating the CNN model for the Nema-App, as depicted in Fig. 11, we aim to increase the accessibility of this method to a broader spectrum of users. Nema-App was developed with Flask in Python, which integrates the trained model of the nematode's photographs.

There are two menus in this application: the Parasitic Menu, which was developed from a previous study by Shabrina *et al.* [30], and the non-parasitic menu, which was deployed from the results of this study. Using the Non-parasitic menu, users can upload nematode microscopy photographs taken from the samples, and the Nema-App annotates the photographs into three feeding types (bacterivore, fungivore, and predator-omnivore). This application also provides a colonizer-persister (c-p) value for the identified sample. The results of this application are shown in Fig. 12. The application can be accessed at https://tinyurl.com/NemaApplication.

## V. Discussion

### A. The Best Performed Model

As demonstrated in Section IV, DenseNet121 achieved the highest test accuracy among the evaluated models. However, its accuracy still fell short of 90%, which may be attributed to the challenging characteristics of the test set. As shown in Fig. 13, the non-parasitic nematode photographs contained considerable background information and a relatively high level of noise, with other objects often appearing close to the primary specimen. These factors likely caused the model to learn spurious patterns from the training data, thereby limiting its ability to generalize. Shabrina *et al.* [31] showed that DenseNet121 did not obtain the best results for plant-parasitic nematodes; however, the same architecture achieved better results for non-parasitic nematodes. This improvement can be attributed to the densely connected convolutional layers of DenseNet121, which facilitate feature reuse and strengthen gradient propagation, thereby enabling the model to capture subtle morphological features while mitigating the effects of background noise. This finding underscores that both the model architecture and dataset characteristics critically influence the classification outcomes. Nevertheless, the presence of noise and previously unseen patterns underscores the necessity of incorporating uncertainty-aware mechanisms in future studies. Such approaches would allow the model to identify low-confidence predictions and refer them for expert validation in the future. This would not only reduce the risk of misclassification when encountering previously unseen genera but also improve overall reliability and potentially facilitate the discovery of novel nematode genera.

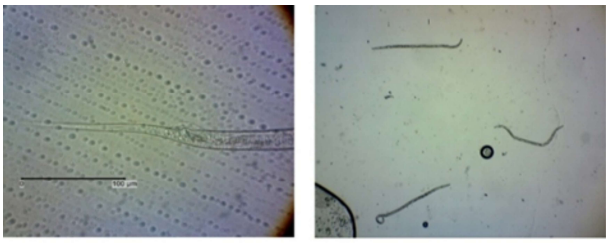

(a) Noise in image (b) Unrelated object in image

Fig. 13. Examples of unrelated features (noise) present in nematode photographs, including bubbles in the object glass, pieces of roots, and plant tissue fragments. These additional objects often appear near the main specimen and can interfere with feature learning by the model.

### B. Comparison of the Predicted Class on the Best Performed Model

This section explains the comparison of the prediction of each class using DenseNet121. The comparison was based on the classification report, which included the precision, recall, and F1-Score derived from the confusion matrix presented in Fig. 14. The precision, recall, and F1-Score for the original and augmented datasets are listed in Table III. The model demonstrated robust and balanced

performance for the bacterivore class, achieving precision, recall, and F1-Score of 0.86, indicating reliable identification with minimal false positives and false negatives. For the fungivore class, the model exhibited lower performance, with a precision of 0.71, recall of 0.62, and an F1-Score of 0.67. These metrics suggest that while the model can reasonably identify true instances of fungivores, it struggles with recall, implying a higher likelihood of missing certain samples. In contrast, the model achieved its best performance for the predator-omnivore class, with a precision of 0.93, recall of 0.95, and an F1-Score of 0.94, reflecting highly accurate and consistent predictions with few classification errors.

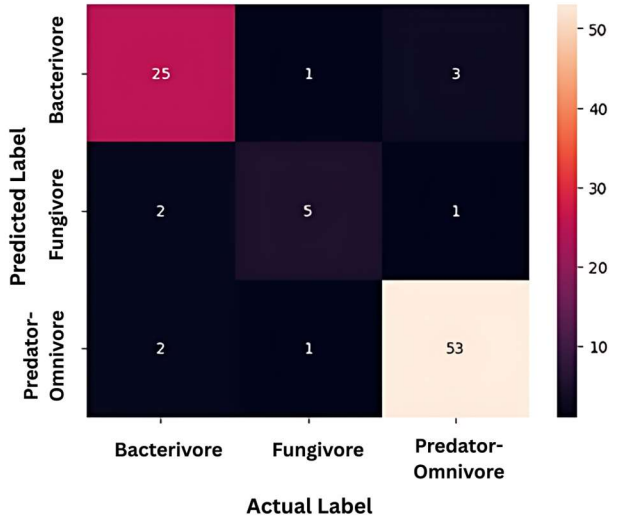


Fig. 14. Confusion matrix of the best-performing model, DenseNet121. The *X*-axis represents the actual nematode classes (bacterivore, fungivore, and predatory-omnivorous), and the *Y*-axis represents the predicted classes. The numbers in each cell indicate the number of samples, and the color intensity corresponds to the frequency of predictions, with darker shades representing lower values and lighter shades representing higher values.

TABLE III. CLASSIFICATION PERFORMANCE OF DENSENET201 ON THE AUGMENTED DATASET

| Class | Dataset type: augmented | | |
|---|---|---|---|
| | Precision | Recall | F1-Score |
| Bacterivore | 0.86 | 0.86 | 0.86 |
| Fungivore | 0.71 | 0.62 | 0.67 |
| Predator-omnivore | 0.93 | 0.95 | 0.94 |

Overall, the model's performance was strongest for the predator-omnivore and bacterivore classes, while the relatively lower performance for the fungivore class may stem from challenges such as a smaller sample size. However, considering the constraints of our dataset size, this score represents a positive outcome. The challenge with small datasets often lies in capturing the complexity and variability of underlying distributions. Despite these limitations, the model's ability to achieve such results demonstrates its capacity for accurate positive predictions. This result is encouraging because it suggests that the model performs well in identifying positive instances. With further data gathering or optimization techniques, there is potential for even greater improvements in performance.

### C. Class Explanation Using the Best Performed Model

The best-performing CNN model was verified through a visualization process employing Gradient-weighted Class Activation Mapping (Grad-CAM) to identify the critical elements in photographs that contributed to the classification. The Grad-CAM approach employs a final convolutional layer to incorporate a harmonious blend of high-level semantic information and precise spatial details into the model's decision-making process [62]. The most significant regions for classification are highlighted using gradients derived from a specific model within the classification network. As depicted in Fig. 15, the output from Grad-CAM for each category displays regions of high and low contribution to the classification, with warm color tones (such as red) indicating a high contribution and cooler tones (such as blue) indicating a low contribution.

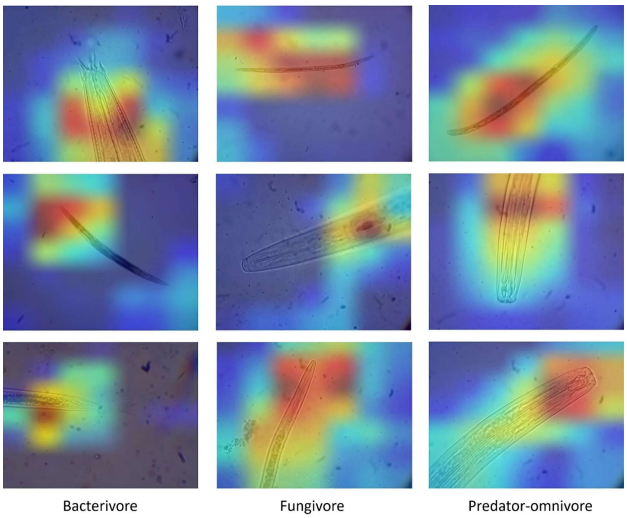


Fig. 15. Grad-CAM visualisation from DenseNet121 trained on original dataset.

The Grad-CAM heatmap results indicated that the model could identify the location of the nematode's body parts rather than the background. However, the heatmap revealed that the model tended to disregard certain features, such as the particular body length of the bacterivore, mouthparts of the fungivore class, and some nematode body parts in the predator-omnivore class. All morphological features are crucial for identifying non-parasitic nematodes based on their feeding habits [11]. Therefore, the model's inability to utilize all the morphological features of the nematode and its tendency to disregard some attributes leads to only moderate performance in classifying non-parasitic nematodes. Further modifications to the model parameters and layers are necessary to improve the performance of the model in classifying non-parasitic nematodes.

### D. Comparison with Other Studies

To the best of our knowledge, this is the first study to provide nematode identification based on feeding type. Considering the focus of this study and the limitations of

the current literature, a comparison was conducted based on the related references. Uhlemann *et al*. [34] showed that Xception resulted in 88.28% accuracy for the juvenile nematode dataset and 69.45% for the adult nematode dataset. Their study also utilized a limited dataset; however, our results surpassed theirs, particularly for the adult datasets. This demonstrates that our approach is better suited for handling small-sized datasets. Lu *et al*. [45] achieved an accuracy rate of 79%. This study used a substantial dataset comprising 2,769 nematode photographs. The results of this study surpass those of their study by employing an even smaller dataset.

Abade *et al*. [33] called NemaNet, successfully achieved 98.88% accuracy using the transfer learning approach. However, this study focused only on soybean phytonematodes and did not focus on other types of nematodes or on identifying their feeding types. Moreover, the study used more photographs consisting of 3063 microscopic photographs with a higher resolution of 5120×3840 pixels and was trained using higher computational resources. In addition, although previous studies reached 98% in terms of test accuracy, the different photograph resolutions prevented the use of the same model, thereby resulting in reduced accuracy [30, 31]. Adding a preprocessing step, such as resizing photographs to a lower resolution while preserving the aspect ratio, applying padding to maintain morphological proportions, or performing background removal to reduce noise, may help lower computational requirements while preserving nematode features and potentially improving the test accuracy.

### *E. Benefits to Ecology*

Sustainable land management and food production rely on the healthy functioning and productivity of soil ecosystems. Regular soil health monitoring is essential for attaining sustainability, and among the most popular methods used by soil ecologists are indices derived from the nematode community structure. The condition of the nematode community structure can be assessed by observing the unbalanced percentage of c-p nematodes. One of the crucial first steps in observing the percentage of c-p nematodes is to identify nematode morphology based on their functional role in the soil ecosystem by categorizing them based on their feeding behavior, namely, bacterivores, fungivores, and predator-omnivores.

The results of this study facilitated the rapid identification and categorization of nematode feeding behavior using input photograph data. Moreover, by employing prototype automatic nematode identification tools, it can also provide the c-p value. This can help nematologists and individuals involved in agricultural activities select the best soil management strategies using the results from the tools. The results from these tools can also serve as important bioindicators to improve soil health and physical or pollution disturbance.

### *F. Limitation and Future Direction*

Although the findings of this study demonstrate the potential of CNN models for non-parasitic nematode identification, several limitations still exist. A primary limitation is the relatively small dataset used for training, which may restrict its generalization to diverse nematode populations. Expanding the dataset with more diverse and representative nematode photographs could significantly enhance the model performance, making it even more effective for broader applications in soil ecosystem management. Another limitation is that the current model does not have the capacity to explicitly flag uncategorized or previously unseen genera. Incorporating uncertainty-aware mechanisms in future studies could enable the model to recognize low-confidence predictions and flag such cases for expert validation, thereby reducing the risk of misclassification and enhancing overall reliability.

Moreover, the dataset employed in this study was curated to include only nematode photographs. The models do not explicitly account for cases in which no nematodes are present. Future work could benefit from incorporating a background or ‘no nematode’ class to better accommodate field-acquired photographs in which specimens may not be present. Finally, this study did not employ stratified k-fold cross-validation owing to computational constraints, as retraining multiple deep CNN architectures across folds would have been prohibitively resource intensive. Future work with greater computational resources should consider this approach to provide a more robust and generalizable performance evaluation.

## VI. Conclusion

In this study, we developed an automated system for identifying non-parasitic nematodes based on their feeding behaviors. The system was trained and tested using a dataset comprising 921 microscopic photographs of non-parasitic nematodes. Ten CNN-based architectures, including Xception, VGG16, ResNet50, InceptionV3, InceptionResNetV2, NASNetMobile, DenseNet121, DenseNet201, EfficientNetV2B0, and ConvNeXtTiny, were implemented and fine-tuned to optimize performance. Among these, DenseNet121 emerged as the top-performing model, achieving a test accuracy of 0.86. Despite this success, the overall accuracy remained below 90%, which can be attributed to the limited size of the dataset, complex morphology of nematodes, and inherent noise in microscopic photographs. Nevertheless, the findings of this study provide a valuable foundation for advancing automated identification systems for non-parasitic nematodes and for further understanding their functional roles in soil ecosystems. In the future, we will focus on refining the CNN architecture using other approaches to improve its performance for non-parasitic nematode classification. We also aimed to extract deeper insights into nematodes by analyzing other aspects at the family or genus level.

## Conflict of Interest

The authors declare no conflict of interest.

## Author Contributions

N. H. S.: Conceptualization, Methodology, Formal

analysis, Investigation, Visualization, Writing—original draft, Project administration, Funding acquisition, Software; L.: Software, Writing—original draft, Visualization; S. I.: Data Curation, Resources, Validation, Writing—review & editing. R. M.: Data Curation, Writing—review & editing. All the authors have read and agreed to the published version of the manuscript.

## ACKNOWLEDGMENT

The first and second authors would like to thank Universitas Multimedia Nusantara for their support during this study. The third and final authors extend their thanks to the Faculty of Agriculture, Universitas Gadjah Mada, for their support during this research. We would also like to thank Gilbert Zaini and Cianando Pautrisio Cendranadi for their help in developing the Nema-App.

## REFERENCES

[1] A. C. Di Montanara, E. Baldrighi, A. Franzo *et al.*, "Free-living nematodes research: State of the art, prospects, and future directions. A bibliometric analysis approach," *Ecol. Inform.*, vol. 72, 101891, 2022. doi: 10.1016/j.ecoinf.2022.101891

[2] T. A. Khanum, N. Mehmood, and N. Khatoon, "Nematodes as biological indicators of soil quality in the agroecosystems," in *Proc. Nematodes: Recent Advances, Management and New Perspectives*, 2022, p. 157. doi: 10.5772/intechopen.99745

[3] Y. Kouser, A. A. Shah, and S. Rasmann, "The functional role and diversity of soil nematodes are stronger at high elevation in the lesser Himalayan Mountain ranges," *Ecol. Evol.*, vol. 11, no. 20, pp. 13793–13804, 2021. doi: 10.1002/ece3.8061

[4] A. Swart, M. Marais, C. Mouton, and G. C. Du Preez, "Non-parasitic, terrestrial and aquatic nematodes," in *Proc. Nematology in South Africa: A View from the 21st Century*, 2017, pp. 419–449. doi: 10.1007/978-3-319-44210-5_20

[5] G. S. Moura and G. Franzener, "Biodiversity of nematodes biological indicators of soil quality in the agroecosystems," *Arq. Inst. Biol.*, vol. 84, e0142015, 2017. doi: 10.1590/1808-1657000142015

[6] A. Ridall and J. Ingels, "Suitability of free-living marine nematodes as bioindicators: Status and future considerations," *Front. Mar. Sci.*, vol. 8, 685327, 2021. doi: 10.3389/fmars.2021.685327

[7] M. Brondani, C. Plassard, E. Ramstein *et al.*, "Morpho-anatomical traits explain the effects of bacterial-feeding nematodes on soil bacterial community composition and plant growth and nutrition," *Geoderma*, vol. 425, 116068, 2022. doi: 10.1016/j.geoderma.2022.116068

[8] J. H. Schmidt, J. Hallmann, and M. R. Finckh, "Bacterivorous nematodes correlate with soil fertility and improved crop production in an organic minimum tillage system," *Sustainability*, vol. 12, no. 17, p. 6730, 2020. doi: 10.3390/su12176730

[9] R. A. Wilschut and S. Geisen, "Nematodes as drivers of plant performance in natural systems," *Trends Plant Sci.*, vol. 26, no. 3, pp. 237–247, 2021. doi: 10.1016/j.tplants.2020.10.006

[10] M. P. Thakur and S. Geisen, "Trophic regulations of the soil microbiome," *Trends Microbiol.*, vol. 27, no. 9, pp. 771–780, 2019. doi: 10.1016/j.tim.2019.04.008

[11] M. Bogale, A. Baniya, and P. DiGennaro, "Nematode identification techniques and recent advances," *Plants*, vol. 9, no. 10, p. 1260, 2020. doi: 10.3390/plants9101260

[12] C. Mulder, A. Boit, M. Bonkowski *et al.*, "A belowground perspective on Dutch agroecosystems: How soil organisms interact to support ecosystem services," *Advances in Ecological Research*, vol. 44, pp. 277–357, 2011. doi: 10.1016/B978-0-12-374794-5.00005-5

[13] L. Alzubaidi, J. Zhang, A. J. Humaidi *et al.*, "Review of deep learning: Concepts, CNN architectures, challenges, applications, future directions," *J. Big Data*, vol. 8, no. 1, p. 53, 2021. doi: 10.1186/s40537-021-00444-8

[14] I. Attri, L. K. Awasthi, T. P. Sharma, and P. Rathee, "A review of deep learning techniques used in agriculture," *Ecol. Inform.*, vol. 77, 102217, 2023. doi: 10.1016/j.ecoinf.2023.102217

[15] A. S. M. M. Hasan, D. Diepeveen, H. Laga, M. G. K. Jones, and F. Sohel, "Image patch-based deep learning approach for crop and weed recognition," *Ecol. Inform.*, vol. 78, 102361, 2023. doi: 10.1016/j.ecoinf.2023.102361

[16] E. Li, L. Wang, Q. Xie, R. Gao, Z. Su, and Y. Li, "A novel deep learning method for maize disease identification based on small sample-size and complex background datasets," *Ecol. Inform.*, vol. 75, 102011, 2023. doi: 10.1016/j.ecoinf.2023.102011

[17] A. A. Salamai, "Enhancing mango disease diagnosis through eco-informatics: A deep learning approach," *Ecol. Inform.*, vol. 77, 102216, 2023. doi: 10.1016/j.ecoinf.2023.102216

[18] A. Vijayalakshmi, V. J. Chakravarthy, and V. Subburaj, "AI and deep learning approach for intelligent and sustainable intensive farming," in *Proc. Innovations in Knowledge Mining: Sustainability for Societal and Industrial Impact*, 2025, pp. 43–53. doi: 10.1007/978-981-96-5217-4_4

[19] S. Albawi, T. A. Mohammed, and S. Al-Zawi, "Understanding of a convolutional neural network," in *Proc. Int. Conf. Eng. Technol. (ICET)*, 2017, pp. 1–6. doi: 10.1109/ICEngTechnol.2017.8308186

[20] Ü. Atila, M. Uçar, K. Akyol, and E. Uçar, "Plant leaf disease classification using EfficientNet deep learning model," *Ecol. Inform.*, vol. 61, 101182, 2021. doi: 10.1016/j.ecoinf.2020.101182

[21] J. Li, Z. Zhu, H. Liu, Y. Su, and L. Deng, "Strawberry R-CNN: Recognition and counting model of strawberry based on improved faster R-CNN," *Ecol. Inform.*, vol. 77, 102210, 2023. doi: 10.1016/j.ecoinf.2023.102210

[22] N. H. Shabrina and A. Brian, "A comparative analysis of pre-trained deep neural networks for mango leaves pests and diseases identification," *ICIC Express Lett., Part B: Appl.*, vol. 14, no. 11, pp. 1207–1215, 2023. doi: 10.24507/icicelb.14.11.1207

[23] A. R. Wang and N. H. Shabrina, "A deep learning-based mobile app system for visual identification of tomato plant disease," *Int. J. Elect. Comput. Eng. (IJECE)*, vol. 13, no. 6, pp. 6992–7004, 2023. doi: 10.11591/ijece.v13i6.pp6992-7004

[24] Z. Wang, Y. Ling, X. Wang *et al.*, "An improved Faster R-CNN model for multi-object tomato maturity detection in complex scenarios," *Ecol. Inform.*, vol. 72, 101886, 2022. doi: 10.1016/j.ecoinf.2022.101886

[25] L. B. Santos, L. M. Bastos, M. F. de Oliveira *et al.*, "Identifying nematode damage on soybean through remote sensing and machine learning techniques," *Agronomy*, vol. 12, no. 10, p. 2404, 2022. doi: 10.3390/agronomy12102404

[26] T. B. Pun, R. Thapa Magar, R. Koech, K. J. Owen, and D. L. Adorada, "Emerging trends and technologies used for the identification, detection, and characterisation of plant-parasitic nematode infestation in crops," *Plants*, vol. 13, no. 21, p. 3041, 2024. doi: 10.3390/plants13213041

[27] Z. Sun, M. Ibrayim, and A. Hamdulla, "Detection of pine wilt nematode from drone images using UAV," *Sensors*, vol. 22, no. 13, p. 4704, 2022. doi: 10.3390/s22134704

[28] T. B. Pun, A. Neupane, and R. Koech, "A deep learning-based decision support tool for plant-parasitic nematode management," *J. Imaging*, vol. 9, no. 11, p. 240, 2023. doi: 10.3390/jimaging9110240

[29] X. Qing, Y. Wang, X. Lu *et al.*, "NemaRec: A deep learning-based web application for nematode image identification and ecological indices calculation," *Eur. J. Soil Biol.*, vol. 110, 103408, 2022. doi: 10.1016/j.ejsobi.2022.103408

[30] N. H. Shabrina, R. A. Lika, and S. Indarti, "Deep learning models for automatic identification of plant-parasitic nematode," *Artif. Intell. Agric.*, vol. 7, pp. 1–12, 2023. doi: 10.1016/j.aiia.2022.12.002

[31] N. H. Shabrina, S. Indarti, R. A. Lika, and R. Maharani, "A comparative analysis of convolutional neural networks approaches for phytoparasitic nematode identification," *Commun. Math. Biol. Neurosci.*, vol. 2023, 2023. doi: 10.28919/cmbn/7993

[32] S. Agarwal, Z. C. Curran, G. Yu *et al.*, "Plant parasitic nematode identification in complex samples with deep learning," *J. Nematol.*, vol. 55, no. 1, 20230045, 2023. doi: 10.2478/jofnem-2023-0045

[33] A. Abade, L. F. Porto, P. A. Ferreira, and F. De B. Vidal, "NemaNet: A convolutional neural network model for identification of soybean nematodes," *Biosyst. Eng.*, vol. 213, pp. 39–62, 2022. doi: 10.1016/j.biosystemseng.2021.11.016

[34] J. Uhlemann, O. Cawley, and T. Kakouli-Duarte, "Nematode identification using artificial neural networks," in *Proc. 1st Int. Conf. Deep Learn. Theory Appl.*, 2020, pp. 13–22. doi: 10.5220/0009776600130022
[35] F. Chollet, "Xception: Deep learning with depthwise separable convolutions," in *Proc. IEEE Conf. Comput. Vis. Pattern Recognit. (CVPR)*, 2017, pp. 1800–1807. doi: 10.1109/CVPR.2017.195
[36] K. Simonyan and A. Zisserman, "Very deep convolutional networks for large-scale image recognition," arXiv Print, arXiv:1409.1556, 2014. doi.org/10.48550/arXiv.1409.1556
[37] K. He, X. Zhang, S. Ren, and J. Sun, "Deep residual learning for image recognition," in *Proc. IEEE Conf. Comput. Vis. Pattern Recognit. (CVPR)*, 2016, pp. 770–778. doi: 10.1109/CVPR.2016.90
[38] C. Szegedy, V. Vanhoucke, S. Ioffe, J. Shlens, and Z. Wojna, "Rethinking the inception architecture for computer vision," in *Proc. IEEE Conf. Comput. Vis. Pattern Recognit. (CVPR)*, 2016, pp. 2818–2826. doi: 10.1109/CVPR.2016.308
[39] C. Szegedy, S. Ioffe, V. Vanhoucke, and A. Alemi, "Inception-v4, inception-ResNet and the impact of residual connections on learning," in *Proc. AAAI Conf. Artif. Intell.*, 2017, pp. 4278–4284.
[40] B. Zoph, V. Vasudevan, J. Shlens, and Q. V. Le, "Learning transferable architectures for scalable image recognition," in *Proc. IEEE/CVF Conf. Comput. Vis. Pattern Recognit.*, 2018, pp. 8697–8710. doi: 10.1109/CVPR.2018.00907
[41] G. Huang, Z. Liu, L. Van Der Maaten, and K. Q. Weinberger, "Densely connected convolutional networks," in *Proc. IEEE Conf. Comput. Vis. Pattern Recognit. (CVPR)*, 2017, pp. 2261–2269. doi: 10.1109/CVPR.2017.243
[42] M. Tan and Q. V. Le, "EfficientNetV2: Smaller models and faster training," in *Proc. 38th Int. Conf. Mach. Learn. (ICML)*, 2021, pp. 10096–10106. doi: 10.48550/arXiv.2104.00298
[43] M. Tan and Q. V. Le, "EfficientNet: Rethinking model scaling for convolutional neural networks," in *Proc. 36th Int. Conf. Mach. Learn. (ICML)*, 2019, pp. 6105–6114.
[44] Z. Liu, H. Mao, C. Y. Wu, C. Feichtenhofer, T. Darrell, and S. Xie, "A ConvNet for the 2020s," in *Proc. IEEE/CVF Conf. Comput. Vis. Pattern Recognit. (CVPR)*, 2022, pp. 11966–11976. doi: 10.1109/CVPR52688.2022.01167
[45] X. Lu, Y. Wang, S. Fung, and X. Qing, "I-Nema: A biological image dataset for nematode recognition," arXiv Print, arXiv:2103.08335, 2021. doi: 10.48550/arXiv.2103.08335
[46] N. Angeline, N. Husna Shabrina, and S. Indarti, "Faster region-based convolutional neural network for plant-parasitic and non-parasitic nematode detection," *Int. J. Elect. Eng. Comput. Sci. (IJEECS)*, vol. 30, no. 1, pp. 316–324, 2023. doi: 10.11591/ijeecs.v30.i1.pp316-324
[47] S. Agarwal, Z. C. Curran, G. Yu *et al.*, "Plant parasitic nematode identification in complex samples with deep learning," *J. Nematol.*, vol. 55, no. 1, 20230045, 2023. doi: 10.2478/jofnem-2023-0045
[48] T. B. Pun, A. Neupane, R. Koech, and K. Walsh, "Detection and counting of root-knot nematodes using YOLO models with mosaic augmentation," *Biosens. Bioelectron.: X*, vol. 15, 100407, 2023. doi: 10.1016/j.biosx.2023.100407
[49] A. Hosna, E. Merry, J. Gyalmo *et al.*, "Transfer learning: A friendly introduction," *J. Big Data*, vol. 9, no. 1, p. 102, 2022. doi: 10.1186/s40537-022-00652-w
[50] D. L. Coyne, J. M. Nicol, and B. Claudius-Cole, *Practical Plant Nematology: A Field and Laboratory Guide*, 3rd ed, Ibadan, Nigeria: International Institute of Tropical Agriculture (IITA), 2018.
[51] G. W. Yeates, T. Bongers, R. G. D. Goede, D. W. Freckman, and S. S. Georgieva, "Feeding habits in soil nematode families and genera-an outline for soil ecologists," *J. Nematol.*, vol. 25, no. 3, pp. 315–331, 1993.
[52] H. Melakeberhan, Z. Maung, I. Lartey *et al.*, "Nematode community-based soil food web analysis of Ferralsol, Lithosol and Nitosol soil groups in Ghana, Kenya and Malawi reveals distinct soil health degradations," *Diversity*, vol. 13, no. 3, p. 101, 2021. doi: 10.3390/d13030101
[53] R. U. Nisa, A. Y. Tantray, N. Kouser *et al.*, "Influence of ecological and edaphic factors on biodiversity of soil nematodes," *Saudi J. Biol. Sci.*, vol. 28, no. 5, pp. 3049–3059, 2021. doi: 10.1016/j.sjbs.2021.02.046
[54] M. Hodda, "Phylum Nematoda: Feeding habits for all valid genera using a new, universal scheme encompassing the entire phylum, with descriptions of morphological characteristics of the stoma, a key, and discussion of the evidence for trophic relationships," *Zootaxa*, vol. 5114, no. 1, pp. 318–451, 2022. doi: 10.11646/zootaxa.5114.1.3
[55] R. A. Lika, N. H. Shabrina, S. Indarti, and R. Maharani, "Transfer learning using hybrid convolution and attention model for nematode identification in soil ecology," *Res. Ideas Outcomes*, vol. 37, no. 4, pp. 945–953, 2023. doi: 10.18280/ria.370415
[56] N. H. Shabrina, R. A. Lika, and S. Indarti, "The effect of data augmentation and optimization technique on the performance of EfficientNetV2 for plant-parasitic nematode identification," in *Proc. IEEE Int. Conf. Ind. 4.0, Artif. Intell., Commun. Technol. (IAICT)*, 2023, pp. 190–195. doi: 10.1109/IAICT59002.2023.10205661
[57] J. Deng, W. Dong, R. Socher *et al.*, "ImageNet: A large-scale hierarchical image database," in *Proc. IEEE Conf. Comput. Vis. Pattern Recognit.*, 2009, pp. 248–255. doi: 10.1109/CVPR.2009.5206848
[58] A. F. Agarap, "Deep learning using Rectified Linear Units (ReLU)," arXiv Print, arXiv:1803.08375, 2019. doi.org/10.48550/arXiv.1803.08375
[59] C. Nwankpa, "Activation functions: Comparison of trends in practice and research for deep learning," arXiv Print, arXiv:1811.03378, 2018. doi: 10.48550/arXiv.1811.03378
[60] Keras. *Keras Applications*. [Online]. Available: https://keras.io/api/applications/
[61] M. Feurer and F. Hutter, "Hyperparameter optimization," in *Proc. Automated Machine Learning*, 2019, pp. 3–33. doi: 10.1007/978-3-030-05318-5_1
[62] R. R. Selvaraju, M. Cogswell, A. Das *et al.*, "Grad-CAM: Visual explanations from deep networks via gradient-based localization," in *Proc. IEEE Int. Conf. Comput. Vis. (ICCV)*, 2017, pp. 618–626. doi: 10.1109/ICCV.2017.74